British Journal of Mathematics & Computer Science
16(5): 1-16, 2016, Article no.BJMCS.26223
ISSN: 2231-0851

SCIENCEDOMAIN *international*
www.sciencedomain.org

SCIENCEDOMAIN

Comparative Design and Analysis of PIDA Controller Using Kitti's and Jung-Dorf Approach for Third Order Practical Systems

D. K. Sambariya[1*] and Deepak Paliwal[1]

[1] *Department of Electrical Engineering, Rajasthan Technical University, Kota 324010, India.*

Authors' contributions

This work was carried out in collaboration between both authors. Author DKS designed the study, performed the statistical analysis, wrote the protocol, and wrote the first draft of the manuscript and managed literature searches. Author DP managed the analyses of the study and literature searches. Both authors read and approved the final manuscript.

Article Information

DOI: 10.9734/BJMCS/2016/26223
Editor(s):
(1) Junjie Chen, Department of Electrical Engineering, University of Texas at Arlington, USA.
Reviewers:
(1) Radek Matusu, Tomas Bata University in Zln, Czech Republic.
(2) Rajendra Prasad Payasi, K N I T, Sultanpur, Uttar Pradesh, India.
Complete Peer review History: http://sciencedomain.org/review-history/14532

Received: 5th April 2016
Accepted: 1st May 2016
Published: 9th May 2016

Original Research Article

Abstract

In this paper, PIDA controller is designed for third-order control systems using Novel Analytical methods. These approaches are based on Jung-Dorf method and Kittis method. This paper demonstrated the PIDA controller design for application of DC motor, Induction motor and AVR power system. The PIDA controller is an extension to the PID controller. The additional term A stands for acceleration, with this new term, a closed-loop system can respond faster with less overshoot. Originally, the PIDA controller design utilizes the Dominant pole concept proceeded in the s-plan.

Keywords: Proportional- Integral- Derivative -Acceleration (PIDA); DC motor; induction motor; Automatic Voltage Regulator (AVR) system.

*Corresponding author: E-mail: dsambariya_2003@yahoo.com;

1 Introduction

In the past decades, the Design of an effective and economic controller is always a non-intuitive and difficult task to control engineers. The PID (proportional-integral-derivative) controller, is widely used in industrial control systems [1]. The most popular design technique is Ziegler-Nichols method [2], which relies solely on parameters obtained from the plant step response. The PID controllers tuned in accordance with the Ziegler-Nichols method have generally a step response with a high percent overshoot. In many control applications, the systems are modeled as a third order. PID controllers are unsuitable, especially for third-order systems. This is the reason that a new structure of the controller becomes the necessity of such systems.

In 1996, Jung and Dorf have proposed a new structure of controller and termed as the proportional-integral-derivative and acceleration (PIDA) controller [3]. This controller has less settling time and over-shoot compared to PID controller for third-order systems. The idea behind the PIDA controller design is to add an extra zero in standard PID controller. Thus, the effect of non-dominant roots is reduced [4]. A New Analytical approach of PIDA design was proposed by Kitti's [5] and extended to discrete system [6].

The application of PIDA was successfully carried out for torsional resonance suppression [4]. Dal-Young et.al, 2001, has used a pre-compensator to PIDA in ac motor [7]. The optimal designs of PIDA controller were presented using Genetic algorithm [8], Harmony search algorithm [9], Firefly algorithm [10] and Bat algorithm [11].

In this paper, the Analytical methods of PIDA controller design are compared. In the beginning, Jung-Dorf approach and Kitti's approach are reviewed briefly. The methods were applied to position control of DC motor, induction motor and AVR system.

The article is organized into four sections. The problem formulation is described in section 2. It includes the design methods and the systems under consideration. The design of PIDA controller for the systems with different approaches is included in section 3. The simulation results with analysis is included in this section. The article is concluded in section 4 and followed by references.

2 Problem Formulation

2.1 Systems for design

2.1.1 Position control of DC motor

As a Reference Armature controlled DC Servo motor can be considered as linear SISO plant model having third-order transfer function. The DC servomotors are found to have an excellent speed and position control [3, 12]. A simple mathematical Relationship between the shaft angular position θ and voltage input V_a to the DC motor may be derived from physical laws.

The dynamic behavior of the armature current-controlled DC servomotor is given by the following equations. The air gap flux ϕ of the motor is proportional to the field current so that

$$\phi = K_f.i_f(t) \tag{2.1}$$

The torque developed by motor is assumed to be related linearly to air gap flux and the armature current as follows:

$$T_m = K_1.\varphi.i_a(t) \tag{2.2}$$

$$T_m = K_1.K_f.i_f(t).i_a(t) \tag{2.3}$$

Where K_1 and K_f are constants. When a constant field current is established in a field coil .The motor torque is

$$T_m = K_m.i_a(t) \tag{2.4}$$

In Laplace transformation

$$T_m = K_m.i_a(s) \tag{2.5}$$

The armature current is related to the input voltage applied to the armature by

$$V_a(s) = R_a I_a(s) + L_a s I_a(s) + V_b(s) \tag{2.6}$$

When $V_b(s)$ is Back E_{mf} voltage proportional to the motor speed. Therefore

$$V_b(s) = K_b \omega(s) \tag{2.7}$$

Where $\omega(s) = s\theta(s)$ the transform of the angular speed and the armature is current is

$$I_a(s) = \frac{V_a(s) - K_b \omega(s)}{R_a + L_a s} \tag{2.8}$$

The motor torque is equal to the torque delivered to the load which may be expressed as

$$T_m(s) = T_l(s) + T_d(s) \tag{2.9}$$

Where T_l is the load torque and T_d is the disturbance torque which is often negligible, so

$$T_l(s) = Js^2\theta(s) + b\, s\, \theta(s) \tag{2.10}$$

Therefore, the transfer function of the motor load combination with $T_d = 0$ is

$$G(s) = \frac{\theta(s)}{V_a(s)} = \frac{K_m}{s(L_a s + R_a)(Js + b) + K_m.K_b)} \tag{2.11}$$

$$G(s) = \frac{\theta(s)}{V_a(s)} = \frac{K_m}{L_a J s^3 + (L_a\, b + R_a J)\, s^2 + (R_a\, b + K_m\, K_b)\, s} \tag{2.12}$$

Here the Angular displacement $\theta(s)$ is considered the output, and the armature voltage $V_a(s)$ is considered the input. The schematic diagram and block diagram representation of DC Motor is shown in Fig. 1 and Fig. 2, respectively. The transfer function parameters given in Table 1.

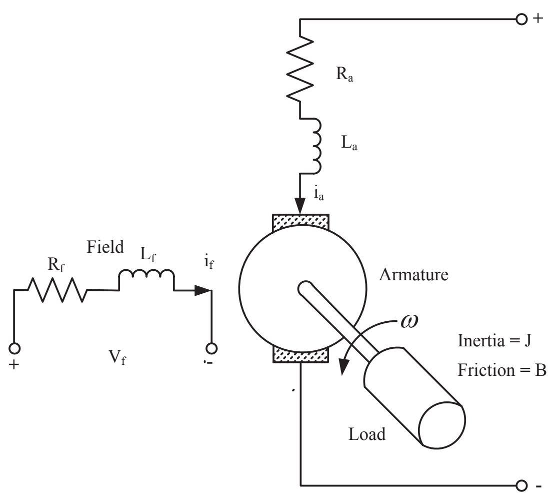

Fig. 1. Schematic diagram separately excited DC motor

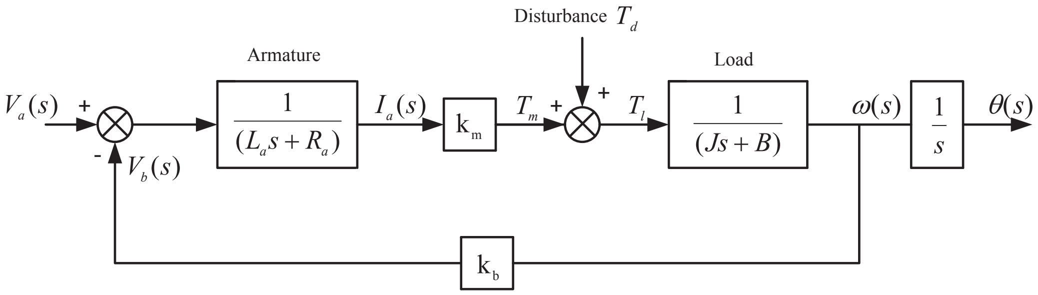

Fig. 2. Block diagram representation of DC motor

Table 1. Parameters of DC motor

S. No.	Parameters	Values
1	Moment of inertia of rotor (J)	$0.01K_gm^2$
2	Motor Viscous friction constant (B)	$0.1Nms$
3	Back emf constant (k_b)	$0.01V/rad/sec$
4	Motor Torque constant (km)	$0.01Nm/Amp$
5	Electric resistance (R_a)	$1.0ohm$
6	Electric inductance (L_a)	$0.5H$

So the transfer function of DC servo motor is as follows:

$$G(s) = \frac{0.01}{0.005s^3 + 0.06s^2 + 0.1001s} = \frac{2}{s^3 + 12s^2 + 20.02s} \tag{2.13}$$

2.1.2 Induction motor

Here PIDA controller is designed for the simplified induction motor position control model that has been implemented in paper [12]. The induction motor model used here is the three phase, star connected, two poles 800 W, 60 Hz, 120 V / 5.4 A. The linearized control structure of induction motor is shown in Fig. 3.

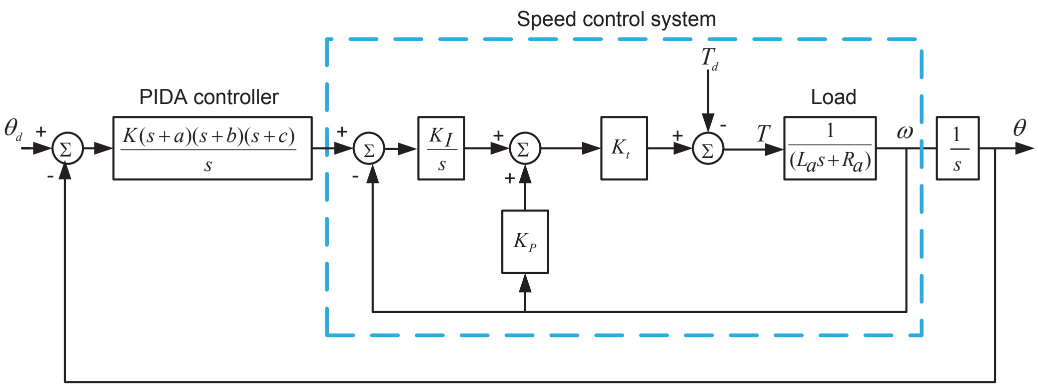

Fig. 3. Block diagram representation of Induction motor

The transfer function of induction motor is given by Eq. 2.14.

$$G(s) = \frac{\theta_d(s)}{\theta(s)} = \frac{K_I K_T}{s(Js^2 + (f + K_P K_t)s + K_I K_t)} \tag{2.14}$$

Where K_P, K_I are PI controller gains and K_t is motor constant. On putting the parameter values

Table 2. Parameters of induction motor

S. No.	Particulars	Values
1	Moment of inertia of rotor (J)	0.305
2	Motor friction (f)	0.2725
3	K_P	14.0242
4	K_I	94.1637
5	K_T	0.5443

as mentioned in Table 2, the transfer function representation of Induction motor can be given as in Eq. 2.15.

$$G(s) = \frac{168.0436}{s(s^2 + 25.921s + 168.0436)} \tag{2.15}$$

2.1.3 Automatic voltage regulator

An automatic voltage regulator (AVR) is commonly used in the generator excitation system of hydro and thermal power plants to regulate generator voltage and control the reactive power flow [13, 9, 10, 14]. The main role of the AVR is to hold the terminal voltage of a synchronous generator at a specified level [11]. The schematic diagram is presented in Fig. 4.

The transfer function representation of the components for AVR power system as followings:

- Amplifier is represented by $\frac{V_r(s)}{V_u(s)} = \frac{K_A}{\tau_A s+1}$
- Exciter is represented by $\frac{V_f(s)}{V_r(s)} = \frac{K_E}{\tau_E s+1}$
- Generator is represented by $\frac{V(s)}{V_f(s)} = \frac{K_G}{\tau_G s+1}$
- Sensor is represented by $\frac{V_s(s)}{V_t(s)} = \frac{K_R}{\tau_R s+1}$

A simple AVR consists of four main components, i.e. amplifier, exciter, generator, and sensor, respectively. A simplified AVR system controlled by the PIDA controller is represented by the block diagram in Fig. 5, where Ve is the error voltage between the reference input voltage $V_{ref}(s)$ and sensor voltage, while V_u, V_r, and V_f are the controlled, amplified, and excited voltage signals, and $V(s)$ is the output voltage. The transfer function AVR System obtained is as follows in Eq. 2.16.

$$G(s) = \frac{250}{s^3 + 13.5s^2 + 37.5s + 25} \tag{2.16}$$

2.2 PIDA design methods

For the control system, the design procedure is as follows:

1. Obtain the mathematical model of plant $G(s)$ as shown in Fig. 6.
2. Obtain the controller $G_c(s)$, such that the desired specifications are acceptable.

Table 3. Parameters of AVR power system

S. No.	Particulars	Values
1	Amplifier gain K_A	10
2	Amplifier time-constant τ_A	0.2725
3	Exciter gain K_E	1.0
4	Exciter time-constant τ_E	0.4
5	Generator gain K_G	1.0
6	Generator time-constant τ_G	1.0
7	Sensor gain K_R	1.0
8	Sensor time-constant τ_R	0.01

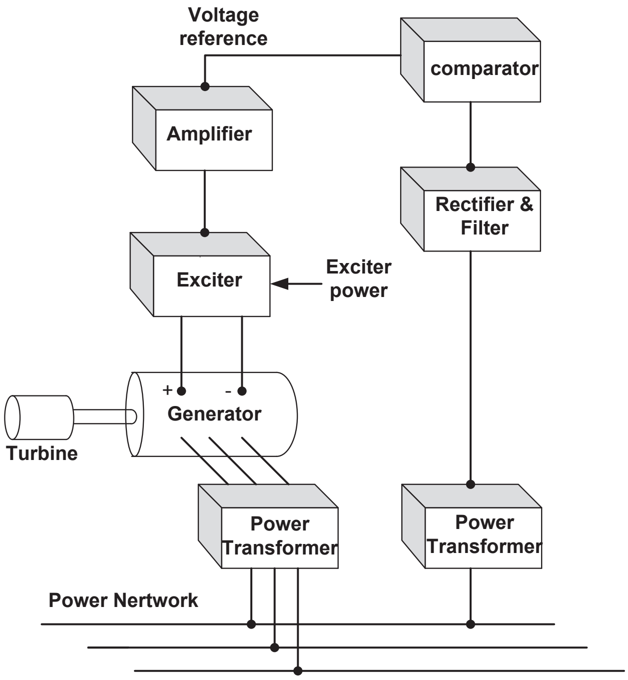

Fig. 4. Schematic diagram of AVR system

The desired specifications necessary for the design of PIDA controller may as following:

- Percent overshoot (PO) given by $e^{\frac{-\zeta\pi}{\sqrt{1-\zeta^2}}} \times 100\%$
- Settling time (T_s) for tolerance of $\pm 2\%$ is given by $-\ln \frac{\left(0.002\sqrt{1-\zeta^2}\right)}{\zeta\omega_n}$

2.2.1 Jung-Dorf approach

The PIDA controller suggested by Jung and Dorf is expressed as mentioned in Eq. 2.17.

$$G_c(s) = K_P + \frac{K_I}{s} + \frac{K_D s}{(s+c)} + \frac{K_A s^2}{(s+d)(s+e)} = K\frac{(s+a)(s+b)(s+c)}{s(s+d)(s+e)} \tag{2.17}$$

Where $a, b, c << d, e$ and two poles (d, e) of PIDA controller are far from the Zeros and excluded in the design for stability consideration. For the closed loop transfer function $T(s)$, the performance is often decided by transient response which includes parameter such as settling time (T_s), percent overshoot (PO) and Peak time (T_p) [3]. Here the set desired specifications are as follows:

- $T_S \leq M$
- $PO \leq L$
- Ratio of disturbance to output max $\left|\frac{C(t)}{D(t)}\right| < W$

The values of L, M and W are selected by the designer. The procedure in designing the PIDA controller in steps as follows:

(i) The dominant roots are q and $\hat{q}$ and the $\hat{q}$ is presented in Eq. 2.18.

$$\hat{q} = -\zeta\omega_n + j\omega_n\sqrt{1-\zeta^2} \tag{2.18}$$

(ii) Determine ζ of the dominant roots from P.O. specification. The ζ is represented as in Eq. 2.19.

$$\zeta = \sqrt{\frac{\left(\ln \frac{L}{100}\right)^2}{\pi^2 + \left(\ln \frac{L}{100}\right)^2}} \tag{2.19}$$

(iii) Select the real root equal to the real part of the dominant roots such as $R = R_e dominant\, roots \leq \zeta\omega_n$. In order to minimize the effect from non-dominant closed loop roots it is suggested to select R, where it is to the left of the largest open loop pole of a plant not at the origin in left half s-plane.

(iv) Select the real root r so that $r << -\zeta\omega_n$

(v) Write the characteristic equation for $1 + G\, G_C = 0$ and set to $(s+r)(s+R)(s+q)(s+\hat{q}) = 0$

(vi) Equate the characteristic equations.

(vii) Solve the simultaneous set of four equations.

(viii) Plot the responses for unity step input.

2.2.2 Kitti's approach

The design of PIDA controller using Kitti's approach follows the following steps:

(i) Obtain the open-loop transfer function of the system as follows in Eq. 2.20.

$$G_c(s)\; G(s) = \frac{K'\;(s+a)\;(s+b)\;(s+c)}{s^2\;(s+\sigma_1)\;(s+\sigma_2)} \tag{2.20}$$

(ii) Set the location of Zero such as $a = \sigma_1 + \Delta\sigma_1$ and $b = \sigma_2 + \Delta\sigma_2$. Only the remaining Zero $(s + c\ )$ and K must be solved for $K = 0, 1, 2, ...$ for the conditions mentioned in Eq. 2.21 and Eq. 2.22.

$$\angle G_C(s)\; G(s) = \pm\; (2k+1)\; \pi \tag{2.21}$$

$$|G_C(s)\; G(s)| = 1 \tag{2.22}$$

(iii) The location of Zero $(s + c)$ can be find from the angle condition at the desired closed loop poles (S_d) as in Eq. 2.23.

$$\angle G_C(s)G(s) = \Sigma\theta_{zero} - \Sigma\theta_{poles} = -180^\circ \tag{2.23}$$

(iv) Compute the magnitude of $zero(c)$ as shown in Fig. 7 and is given in Eq. 2.24.

$$\mathrm{c} = |\mathrm{Re(s_d)}| + \frac{|\mathrm{Img(s_d)}|}{\tan(\hat{\mathrm{c}}^\circ)} \tag{2.24}$$

(v) Compute the open loop gain from the magnitude condition.

(vi) Compute the PIDA controller parameters.

(vii) Plot the closed loop unit step response of the system.

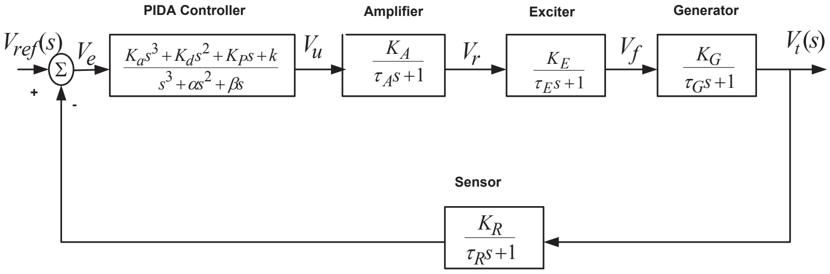

Fig. 5. Control block diagram of AVR system

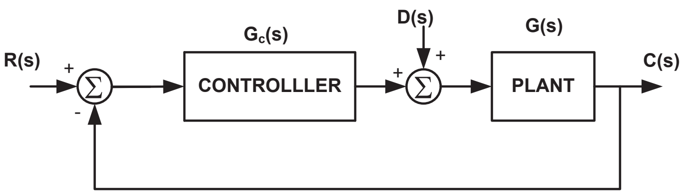

Fig. 6. Representation of control structure

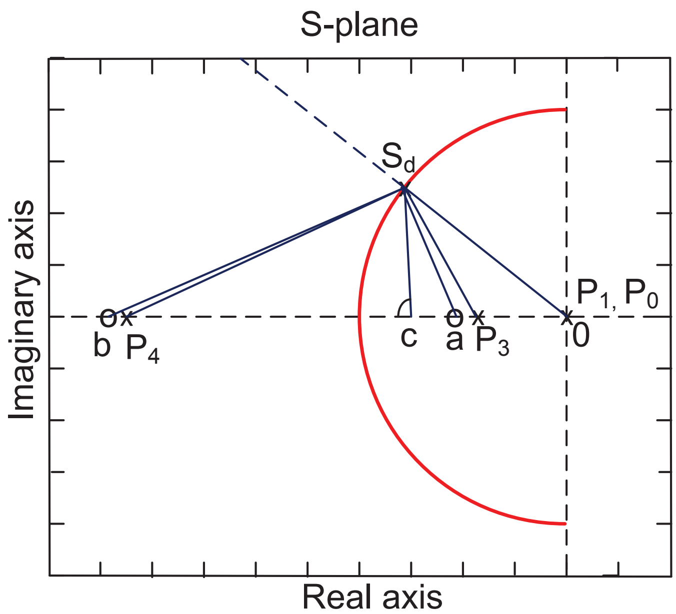

Fig. 7. Determination of the angle of $zero(s + c)$

3 Design and Simulation Results

3.1 DC motor

3.1.1 Design using Jung-Dorf approach

The transfer function of DC servo motor is shown in Eq. 2.13. The procedure for designing the PIDA controller already mentioned in previous section.

- Considering the settling time as $T_s = \frac{4}{\zeta\omega_n} \leq -2$. The dominant roots are given by $q, \hat{q} = -\zeta\omega_n \pm j\omega_n\sqrt{1-\zeta^2} = -2.118 \pm j2.221$.
- Determine ζ of the dominant roots from PO specification are found such as $\zeta = \sqrt{\frac{(\ln\frac{L}{100})^2}{\pi^2+(\ln\frac{L}{100})^2}} \geq 0.707$.
- Select the real root equal to the real part of the dominant roots using, $R = R_e\, dominant\, roots \leq \zeta\omega_n = -2.118$.
- Select the real root r so that $r << -\zeta\omega_n$ i.e. for this system $r = -30$.
- Write the characteristic equation for $1+G\, G_C = 0$ and set as $(s+r)(s+R)(s+q)(s+\hat{q}) = 0$.

$$1+G(s)G_c(s) = s^4+(12+K)s^3+[K(a+b+c)+20.02]s^2+K(ab+bc+ca)s+Kabc = 0 \quad (3.1)$$

$$(s+r)(s+R)(s+q)(s+\hat{q}) = (s+2.2)(s+30)(s+2.118+2.221j)(s+2.118-2.221j) = 0 \quad (3.2)$$

- Equate the characteristic equations.
- Solve the simultaneous set of four equations.

$$12 + K' = 36.354 \quad (3.3)$$

$$K'(a+b+c) + 20.02 = 209 \quad (3.4)$$

$$K'(ab + c(a+b)) = 571.668 \quad (3.5)$$

$$K'abc = 598.47 \quad (3.6)$$

- Solving Eq. 3.3 - Eq. 3.6 for a, b, c and K yields, $a = 2.8003+j1.8822$, $b = 2.8003+j1.8822$, $c = 2.1585$, $K = 24.354$, $K = 12.177$. The transfer function of the controller can be written as in Eq. 3.7.

$$G_c = \frac{12.177(s^3 + 7.76s^2 + 23.472s + 24.572)}{s} \quad (3.7)$$

- The step responses of the plant with PIDA controller is shown in Fig. 8 and the step response information such as settling time, peak time, etc. are shown in Table 4.

3.1.2 Design using Kitti's approach

The procedural steps are already mentioned in section 2.2.2. In this section the PIDA controller is designed using Kitti's method as following:

- The open-loop transfer function of the system is given by Eq. 3.8.

$$G_c(s)G(s) = \frac{K'(s+a)(s+b)(s+c)}{s^2(s+9.9975)(s+2.0025)} \quad (3.8)$$

- Set the location of zeros such as $a = 10.0975$ and $b = 2.1025$. The remaining Zeros associated to $(s+c)$ and K must be solved using Eq. 3.9 and Eq. 3.10.

$$\angle G_C(s)G(s) = \pm(2k+1)\pi \quad (3.9)$$

$$|G_C(s)G(s)| = 1 \quad (3.10)$$

- The location of zero of $(s + c)$ can be find from the angle condition at the desired dominant closed loop poles $s_d = -\xi\omega_n \pm j\omega_n\sqrt{1-\xi^2} = -2.118 + i2.221$. The angle condition at the desired closed loop poles (S_d) as follows:

$$\angle G_C(s)G(s) = \Sigma\theta_{zero} - \Sigma\theta_{poles} = -180^\circ \tag{3.11}$$

$$\angle G_C(s)G(s) = \angle \frac{K(s_d + a)(s_d + b)(s_d + c)}{(s_d)^2(s_d + 9.9975)(s_d + 2.0025)} \tag{3.12}$$

$$\Sigma\theta_{zero} = \angle(s_d + a) + \angle(s_d + b) + \angle(s_d + c) = 15.554^\circ + 90.399^\circ + \hat{c} = 105.953^\circ + \hat{c}^\circ \tag{3.13}$$

$$\begin{aligned}\Sigma\theta_{poles} &= \angle(s_d) + \angle(s_d) + \angle(s_d + 9.9975) + \angle(s_d + 2.0025)\\ &= 133.64^\circ + 133.64^\circ + 15.726^\circ + 92.977^\circ\\ &= 375.983\end{aligned} \tag{3.14}$$

$$\begin{aligned}&\Sigma\theta_{zero} - \Sigma\theta_{poles} = -180^\circ\\ &105.953^\circ + \hat{c} - 375.983^\circ = -180^\circ\\ &\hat{c} = 90.03^\circ\end{aligned} \tag{3.15}$$

- Compute the magnitude of Zero(c) as follows:

$$\mathrm{c} = |\mathrm{Re(s_d)}| + \frac{|\mathrm{Img(s_d)}|}{\tan\hat{c}^\circ} = 2.118 + \frac{2.221}{\tan(90.03^\circ)} = 2.1168 \tag{3.16}$$

- Open loop Gain K can be find from magnitude condition.

$$\left|\frac{K'(s_d + a)(s_d + b)(s_d + c)}{(s_d)^2(s_d + 9.9975)(s_d + 2.0025)}\right| = 1 \tag{3.17}$$

$$\left|\frac{K' \times 8.2852 \times 2.221 \times 2.1168}{3.07 \times 3.07 \times 8.194 \times 2.224}\right| = 1 \tag{3.18}$$

$$\begin{aligned}K' &= 4.411\\ K &= \tfrac{K'}{475.836} = 9.27 \times 10^{-3}\end{aligned} \tag{3.19}$$

- The PIDA controller transfer function can be given as following in Eq. 3.20.

$$G_c(s) = \frac{9.27 \times 10^{-3}(s + 10.0975)(s + 2.1025)(s + 2.1168)}{s} \tag{3.20}$$

- The step responses of the plant with PIDA controller is shown in Fig. 8 and the step response information such as settling time, peak time, etc. are shown in Table 4.

3.1.3 Simulation results

The circuit for simulation in MATLAB is Considered as shown in Fig. 6, where, $G(s)$ stands for the transfer function of DC motor as in Eq. 2.13 and $G_c(s)$ stands for the transfer function of PIDA controller determined using Jung-Dorf method and Kitti's method as presented in Eq. 3.7 and Eq. 3.20, respectively. The combination of DC motor with PIDA controller is subjected to simulation on application of step input. The response of the system (DC Motor) without controller, with PIDA controller using Jung-Dorf approach and with PIDA using Kitti's approach are compared and shown in Fig. 8. The step response data are enlisted in Table 4.

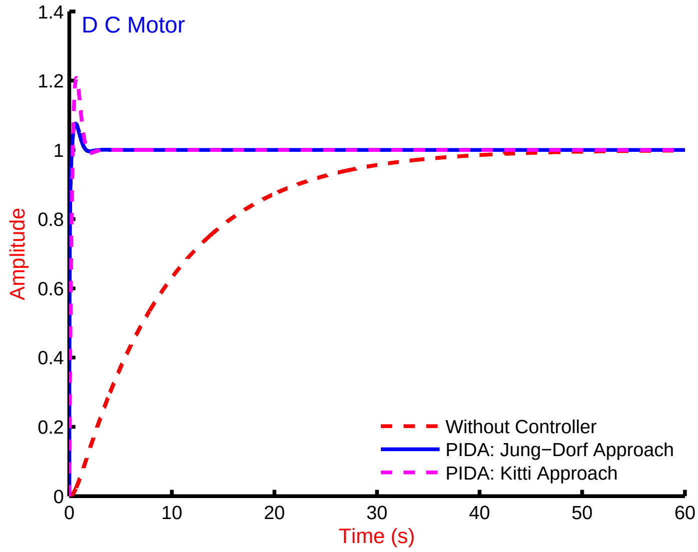

Fig. 8. Step response comparison of DC servo motor without controller, with PIDA controller using Jung-Dorf method and Kitti's method

Table 4. Step response information of DC motor with PIDA controller based on Jung-Dorf and Kitti's approaches

S. No.	Particulars	Jung-Dorf approach	Kitti's approach
1	Rise Time (s)	0.1320	0.2676
2	Settling Time (s)	1.2731	1.5503
3	Overshoot	7.5958	20.7875
4	Peak	1.0760	1.2079
5	Peak Time (s)	0.6359	0.7088

3.2 Induction motor

3.2.1 Design using Jung-Dorf approach

The transfer function of induction motor have been presented in Eq. 2.15. The theoretical development to determine the PIDA controller using Jung-Dorf approach is presented in section 2.2.1. The similar steps are considered to determine the PIDA controller for Induction motor as presented in section 3.1.1. The PIDA controller found for the Induction motor is presented in Eq. 3.21.

$$G_c = \frac{0.1268(s^3 + 19.4016s^2 + 96.517s + 172.3565)}{s} \tag{3.21}$$

3.2.2 Design using Kitti's approach

The design aspects of the PIDA controller for induction motor using Kitti's approach is considered in this section. The theoretical development to determine the PIDA controller using Kitti's approach is presented in section 2.2.2. The similar steps are considered to determine the PIDA controller for Induction motor as presented in section 3.1.2. The such obtained PIDA controller for the Induction motor is presented in Eq. 3.22.

$$G_c(s) = \frac{0.0248\,(s^3 + 28.3356s^2 + 228.516s + 378.081)}{s} \tag{3.22}$$

3.2.3 Simulation results

Considering the arrangement as shown in Fig. 6, where, $G(s)$ stands for the transfer function of Induction motor (as in Eq. 2.15) and $G_c(s)$ stands for the transfer function of PIDA controller determined Jung-Dorf method as presented in Eq. 3.21. The combination of Induction motor with PIDA controller is subjected to simulation on application of step input. The response of the system (Induction motor) without controller and with PIDA controller (based on both approaches) are compared and shown in Fig. 9.

Table 5. Step response information of induction motor with PIDA controller based on Jung-Dorf and Kitti's approaches

S. No.	Particulars	Jung-Dorf approach	Kitti's approach
1	Rise Time (s)	0.1809	0.2776
2	Settling Time (s)	1.3831	1.5854
3	Overshoot	9.4835	21.3939
4	Peak	1.0948	1.2139
5	Peak Time (s)	0.6710	0.7475

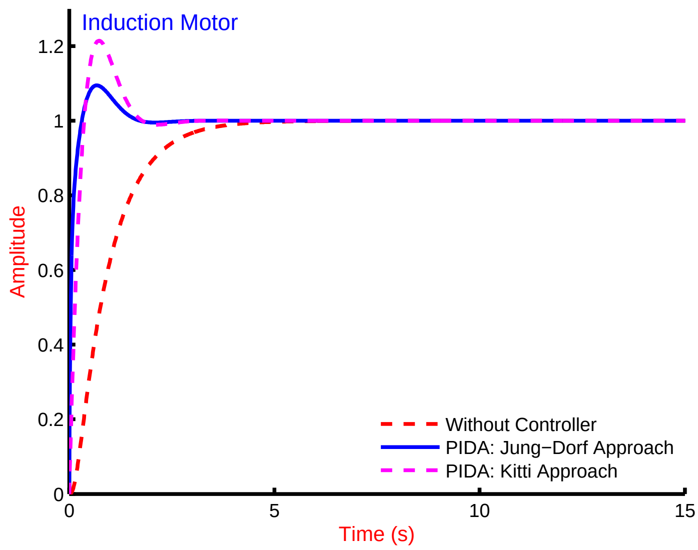

Fig. 9. Step response comparison of induction motor without controller, with PIDA controller using Jung-Dorf method and Kitti's method

3.3 AVR power system

3.3.1 Design using Jung-Dorf approach

The transfer function of AVR power system have been presented in Eq. 2.16. The theoretical development to determine the PIDA controller using Jung-Dorf approach is presented in section 2.2.1. The similar steps are considered to determine the PIDA controller for Induction motor as presented in section 3.1.1. The PIDA controller found for the AVR power system is presented in Eq. 3.23.

$$G_c = \frac{0.0914(s^3 + 7.5041s^2 + 23.9204s + 26.1866)}{s} \quad (3.23)$$

3.3.2 Design using Kitti's approach

The design aspects of the PIDA controller for AVR power system using Kitti's approach is considered in this section. The theoretical development to determine the PIDA controller using Kitti's approach is presented in section 2.2.2. The similar steps are considered to determine the PIDA controller for AVR power system as presented in section 3.1.2. The such obtained PIDA controller for the AVR power system is presented in Eq. 3.24.

$$G_c(s) = \frac{0.0107(s^3 + 15.495s^2 + 61.756s + 73.396)}{s} \quad (3.24)$$

3.3.3 PID controller

In this section, PID controller using Ziegler Nichols method is designed and mentioned in Eq. 3.25 [15].

$$G_c(s) = \frac{5s^2 + 8s + 8.66}{0.002s^5 + 0.067s^4 + 0.615s^3 + 6.55s^2 + 9s + 8.66} \quad (3.25)$$

3.3.4 Simulation results

The $G(s)$ stands for the transfer function of AVR power system as in Eq. 2.16 and $G_c(s)$ stands for the transfer function of PIDA controller determined using Jung-Dorf method and Kitti's method as presented in Eq. 3.23 and Eq. 3.24, respectively. The combination of AVR power system with PIDA controller is subjected to simulation on application of step input. The response of the system (AVR power system) without controller, with PIDA controller using Jung-Dorf approach and with PIDA using Kitti's approach are compared and shown in Fig. 10. The step response data are enlisted in Table 6. The step response of the system without controller, with PIDA controller using both techniques and with PID controller [15] are comapred in Fig. 11 and the information is included in the Table 6. The response of AVR power system outperforms that of with PIDA controller as compared to that of with PID controller.

Table 6. Step response information of AVR power system with PIDA controller based on Jung-Dorf and Kitti's approaches and with PID controller [15]

S. No.	Particulars	Jung-Dorf approach	Kitti's approach	PID controller
1	Rise Time (s)	0.1714	0.4091	0.1550
2	Settling Time (s)	1.2532	1.7670	2.7318
3	Overshoot	4.0376	14.2295	23.6915
4	Peak	1.0404	1.1423	1.2369
5	Peak Time (s)	0.7723	0.9713	0.3620

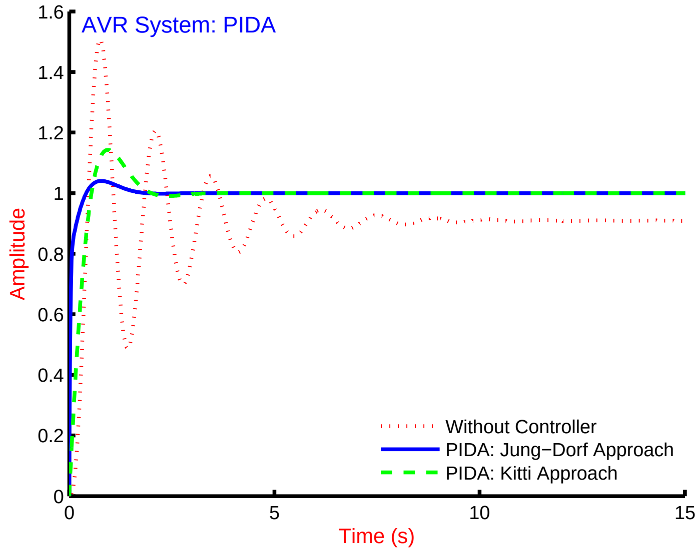

Fig. 10. Step response comparison of Automatic Voltage Regulator (AVR) power system without controller, with PIDA controller using Jung-Dorf method and Kitti's method

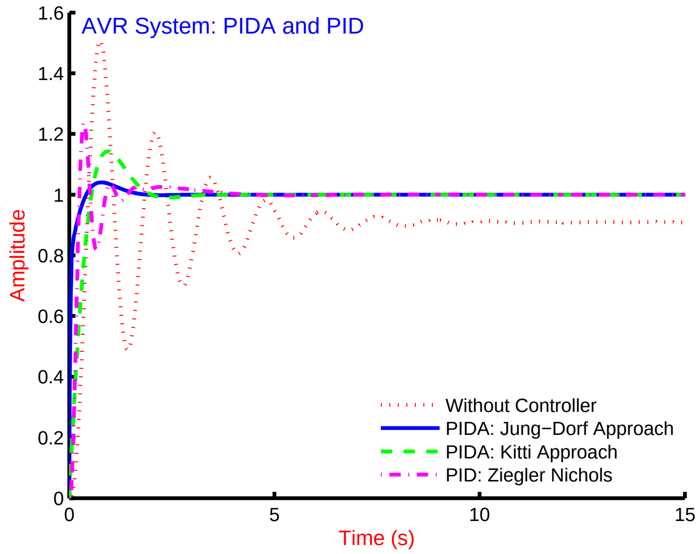

Fig. 11. Step response comparison of AVR system without controller, with PIDA controller using Jung-Dorf method and Kitti's method and PID based on Ziegler-Nichols method [15]

4 Conclusion

The Analytical methods of PIDA controller design are compared. In this paper, three practical systems such as DC Motor, Induction motor and automatic voltage regulator (AVR), are considered for the optimal design of PIDA controller using Kitti's Approach and Jung-Dorf approach. The Kitti's Approach of PIDA design has appeared with more over-shoots as compared to Jung-Dorf approach. Both approaches have better steady-state characteristics than the system with PID controller [15].

Competing Interests

Authors have declared that no competing interests exist.

References

[1] Sambariya DK, Prasad R. Design of robust PID power system stabilizer for multimachine power system using HS algorithm. American Journal of Electrical and Electronic Engineering. 2015;3(3):75-82.
DOI: 10.12691/ajeee-3-3-3
Available: http://dx.doi.org/10.12691/ajeee-3-3-3

[2] Ziegler JG, Nichols NB. Optimum settings for automatic controllers. J. Dyn. Sys., Meas., Control. 1993;115(2B):220-222.
DOI: 10.1115/1.2899060
Available: http://dx.doi.org/10.1115/1.2899060

[3] Jung S, Dorf R. Analytic PIDA controller design technique for a third order system. In: Proceedings of the 35th IEEE Conference on Decision and Control, (CDC-1996). 1996;3:2513-2518.
DOI: 10.1109/CDC.1996.573472
Available: http://dx.doi.org/10.1109/CDC.1996.573472

[4] Puangdownreong D. Application of current search to optimum PIDA controller design. Intelligent Control and Automation. 2012;3(0):303-312.
DOI: 10.4236/ica.2012.34035
Available: http://dx.doi.org/10.4236/ica.2012.34035

[5] Ukakimaparn P, Pannil P, Boonchuay P, Trisuwannawat T. PIDA controller designed by kitti's method. In: ICCAS-SICE. 2009;1547-1550.

[6] Smerpitak K, Ukakimaparn P, Trisuwannawat T, La-orsri P. Discrete-time PIDA controller designed by kitti's method with bilinear transform. In: Control, Automation and Systems (ICCAS), 2012 12th International Conference on. 2012;1585-1590.

[7] Dal-Young H, Ihn-Yong L, Young-Seung C, Young-Do L, Boo-Kwi C. The design of PIDA controller with pre-compensator [for induction motors. In: Proceedings. ISIE 2001, IEEE International Symposium on Industrial Electronics. 2001;2:798-804.
DOI: 10.1109/ISIE.2001.931570
Available: http://dx.doi.org/10.1109/ISIE.2001.931570

[8] Sornmuang S, Sujitjorn S. Ga-based optimal PIDA controller design. In: Proceedings of the 10th WSEAS International Conference on Systems theory and Scientific Computation. World Scientific and Engineering Academy and Society (WSEAS). 2010;192-197.

[9] Sambariya DK, Paliwal D. Optimal design of PIDA controller using harmony search algorithm for avr power system. In: 6^{th} IEEE International Conference on Power Systems, (ICPS-2016). 2016;1-6.

[10] Sambariya DK, Paliwal D. Optimal design of PIDA controller using firefly algorithm for avr power system. In: International Conference on COMPUTING COMMUNICATION AND AUTOMATION (ICCCA-2016). 2016;1-5.

[11] Sambariya DK, Paliwal D. Design of pida controller using bat algorithm for avr power system. Advances in Energy and Power. 2016;4(1):1-6.
DOI: 10.13189/aep.2016.040101
Available: http://dx.doi.org/10.13189/aep.2016.040101

[12] Liaw GM, Lin FJ. A robust speed controller for induction motor drives. IEEE Transactions on Industrial Electronics. 1994;41(3):308-315.
DOI: 10.1109/41.293901
Available: http://dx.doi.org/10.1109/41.293901

[13] Nath V, Sambariya DK. Analysis of AGC and AVR for single area and double area power system using fuzzy logic control. International Journal of Advanced Research in Electrical, Electronics and Instrumentation Engineering. 2015;4(7):6501-6511.
DOI: 10.15662/ijareeie.2015.0407075.
Available: http://dx.doi.org/10.15662/ijareeie.2015.0407075

[14] Sambariya DK, Nath V. Optimal control of automatic generation with automatic voltage regulator using particle swarm optimization. Universal Journal of Control and Automation. 2015;3(4):63-71.
Available: http://dx.doi.org/10.13189/ujca.2015.030401

[15] Madasamy G, Ravichandran CS. PID controller tuning optimization with BFO algorithm in AVR system. International Journal on Recent and Innovation Trends in Computing and Communication. 2014;2(2):3823-3827.

Peer-review history:
The peer review history for this paper can be accessed here (Please copy paste the total link in your browser address bar)
http://sciencedomain.org/review-history/14532